

Article

Application of *Shewanella xiamenensis* Placed on Zeolite in Treatment of Silver-Containing Effluents

Inga Zinicovscaia ^{1,2,*} , Nikita Yushin ¹ , Dmitrii Grozdov ¹  and Alexey Safonov ³ ¹ Joint Institute for Nuclear Research, Joliot-Curie Str., 6, 141980 Dubna, Russia² Horia Hulubei National Institute for R&D in Physics and Nuclear Engineering, 30 Reactorului Str., 077125 Bucharest, Romania³ Frumkin Institute of Physical Chemistry, Russian Academy of Science, 31 Leninsky Prospect, GSP-1, 119071 Moscow, Russia

* Correspondence: zinicovskaia@mail.ru; Tel.: +7-496-216-5609

Abstract: The adsorption properties of *Shewanella xiamenensis* immobilized on zeolite have been evaluated in order to determine its applicability for remediation of silver-containing effluents with different chemical composition. The effects of pH (2.0–6.0), contact time (15–150 min), silver concentration (10–100 mg/L) and temperature (20–50 °C) on the bio-zeolite adsorption efficiency were investigated in batch experiments. The optimal pH for metal ions removal was in the range of 4.0–6.0, while the time required to attained equilibrium lay between 60 and 150 min. The adsorption of silver was described by a pseudo-second-order kinetic model in Ag- and Ag-Cu-Ni-Zn systems, while in Ag-Cu systems, it fitted well the pseudo-first-order kinetic model. The maximum adsorption capacities of silver on bio-zeolite calculated from the Langmuir model were 14.8 mg/g (Ag system), 32.5 mg/g (Ag-Cu system) and 12.8 mg/g (Ag-Cu-Ni-Zn system). The thermodynamic parameters showed that the adsorption of metal ions onto bio-zeolite was a spontaneous entropy-driven process.

Keywords: bio-zeolite; copper; nickel; zinc; remediation; *Shewanella xiamenensis*

Citation: Zinicovscaia, I.; Yushin, N.; Grozdov, D.; Safonov, A. Application of *Shewanella xiamenensis* Placed on Zeolite in Treatment of Silver-Containing Effluents. *Minerals* **2023**, *13*, 179. <https://doi.org/10.3390/min13020179>

Academic Editor: Javier Sánchez-España

Received: 8 January 2023

Revised: 23 January 2023

Accepted: 23 January 2023

Published: 26 January 2023



Copyright: © 2023 by the authors. Licensee MDPI, Basel, Switzerland. This article is an open access article distributed under the terms and conditions of the Creative Commons Attribution (CC BY) license (<https://creativecommons.org/licenses/by/4.0/>).

1. Introduction

Silver along with gold and the six platinum-group metals are referred to as precious metals [1]. Due to its excellent malleability, non-corrosive nature, photosensitivity as well as antimicrobial properties, silver and its compounds are widely applied in medicine, electroplating, electronic and chemical industries, agriculture and jewellery production [1,2]. Annually, approximately 2500 tons of industrial waste are generated and emitted containing silver along with other metal ions, of which 150 tons enter wastewater treatment plants and 80 tons are released into surface waters [3]. In addition to different silver compounds, at present, the use of silver in nanoform has been gathering steam. It is considered that approximately 320 tons of silver nanoparticles are produced every year and used in different fields of medicine and industry [4]. Besides silver's importance for industry, it is crucial to highlight its toxicity for living organisms. Silver ions along with cadmium, chromium (VI), copper, and mercury belong to chemical elements with the highest toxicity [3]. The toxicity of silver in different forms is described in detail in many papers [5–8].

The recovery of silver from industrial wastewater is of practical importance due to silver resources limitations and its environmental impact [9,10]. Currently, methods such as chemical precipitation, electrochemical deposition, ultra-filtration, reverse osmosis, ion exchange and membrane separation are used for removal of silver ions from wastewater [11–13]. Often these techniques have serious operation shortcomings, such as, for example, high energy consumption, poor selectivity, high cost, secondary pollution and generation of toxic sludge, which require disposal and further treatment [11,12,14]. Among these methods, adsorption, and especially biosorption, have won a special place due to several critical advantages, such as low cost, high sorption capacity, simple operation, the

possibility of application for treatment of complex wastewater, no secondary pollution and regeneration of biosorbents [12,15,16].

Biosorption of heavy metals by bacterial biomass (living or dead biomass) has been the subject of significant research interest in recent decades. Bacteria's large application in metal removal is explained by their omnipresence, ability to adapt to high levels of heavy metal pollution, ability to grow under controlled conditions, and resistance to a wide range of environmental conditions [17–19]. However, the free bacterial cells are basically small particles, with low density and poor mechanical strength, which may create problems during their industrial application. It is well known that removal of free suspended bacteria from the purified effluent is one of the most important challenges during the treatment process [20]. One of the optimal approaches to avoiding this problem is immobilization of the microbial biomass in solid structures [19]. The selection of the matrix is critically important in the environmental application of immobilized biomass. The main type of matrices used for microorganisms immobilization are listed in review papers [19,21]. However, the common matrices such as alginate and polyacrylamide are characterized by low stability and toxicity, respectively [20].

Zeolites, naturally occurring crystalline aluminosilicate, proved to be efficient sorbents for metal removal [22–24]. Zeolite, due to its low cost and resistance to microbial degradation, can be considered an ideal matrix applied for the immobilization of microorganisms [20]. In the wastewater treatment process, the cultivation of bacteria assimilated to the composition of effluents influences the efficiency of the treatment process [25] and the use of zeolite as support for microbial biomass growth can significantly increase the efficacy of the removal process [26] and reduction of the time of sorption [27].

Escherichia coli biofilm placed on zeolite was able to remove 54.61% of copper and 57.35% of zinc ions from wastewater [28]. *Rhododendron viscosum* supported on zeolite was successfully performed and the removal rates were 85% for copper, 95% for zinc and 25% for atrazine from wastewater [29]. Application of aerobic biomass biofilm supported on untreated clinoptilolite zeolite for reduction of the concentration of copper from synthetic solutions was reported by [30]. The biosorption capacity of biofilm of *Escherichia coli* supported on NaY zeolite followed the sequence: Fe(III) > Ni(II) > Cd(II) > Cr(VI) [31].

To our knowledge, there is no information about silver ions removal using microbial biofilm formed onto a support material. The aim of the present study was to examine sorption properties of *Shewanella xiamenensis* biofilm formed on zeolite (bio-zeolite) for treatment of silver-containing effluents. To achieve the goal of the study, the effect of several parameters on bio-zeolite sorption capacity was investigated. Kinetic, equilibrium and thermodynamic studies were performed in order to understand the nature of the biosorption process.

2. Materials and Methods

2.1. Effluents

To prepare synthetic effluents, chemicals of analytical grade purchased from Sigma-Aldrich (Darmstadt, Germany) were used. Three effluents with the following composition: Ag, Ag-Cu and Ag-Cu-Ni-Zn were studied. The elemental composition of the effluents as well as used metal concentrations are presented in Table 1.

Table 1. Chemical composition and metal concentrations in prepared synthetic effluents.

System	Concentration, mg/L			
	Ag	Cu	Ni	Zn
Ag	10 ± 0.4	-	-	-
Ag-Cu	10 ± 0.3	5 ± 0.06	-	-
Ag-Cu-Ni-Zn	10 ± 0.3	5 ± 0.06	2 ± 0.01	2 ± 0.02

Silver application in the electroplating process, in the production and use of silver-copper containing plastic plates leads to the generation of wastewater containing silver along with copper, nickel and other metal ions [32]. This fact influenced the choice of synthetic effluents elemental composition.

2.2. Preparation of Biosorbent

Bacteria *Shewanella xiamenensis* DCB2-1 (*S. xiamenensis*) were isolated from a ground-water sample obtained near a suspended surface repository for radioactive waste in Russia. A detailed description of the strain can be found in [33]. Zeolite with the following composition: 65.2% of clinoptilolite, 1.5% of cancrinite, 22.7% of heulandite (Na) and 12.1% of heulandite (Ca) was obtained from the Chola deposit (Chita Region, Russia). The characteristics of zeolite are given in [27].

To obtain biofilm on the zeolite, on the third day of bacteria growth, 50 g of zeolite, with the size in the range of 100–300 μm , was introduced to the 250 mL of inoculum, and the biomass was grown until the seventh day. At the end of the experiment, the obtained biosorbent was separated from the cultivation medium by filtration, freeze-dried (ScanVac CoolSafe, LaboGene, Frederiksborg, Denmark, <https://www.labogene.com/CoolSafe-4-15-L-Freeze-Dryers>, accessed on 25 January 2023) and used for further experiments.

2.3. Experiment Design

In biosorption experiments, the effect of pH (2.0–6.0), silver ions concentration (10–100 mg/L), time of contact (15–180 min) and temperature (20–50 $^{\circ}\text{C}$) on biosorbent removal capacity were investigated. All experiments were performed in 100 mL flasks, containing 50 mL of solution and 0.5 g of sorbent at continuous agitation at 200 rpm (Unimax 1010, Heidolph, Schwabach, Germany). All experiments, except thermodynamic studies, were carried out at room temperature. The pH of the solutions was adjusted using NaOH or HNO₃ (Sigma-Aldrich, Darmstadt, Germany). In equilibrium experiments, the concentrations of copper, zinc and nickel ions were maintained constantly. All experiments were performed in triplicate and each value represents the mean of three test runs.

The sorption capacity of obtained biosorbent q (mg/g) was calculated from Equation (1):

$$q = \frac{V(C_i - C_f)}{m} \quad (1)$$

and the efficiency of metal ions removal, E (%), using Equation (2):

$$E = \frac{C_i - C_f}{C_i} \times 100 \quad (2)$$

where V is the volume of the solution in mL, C_i and C_f are the initial and final metal ions concentrations, mg/L, and m is the mass of sorbent, g.

2.4. Applied Techniques

The efficiency of metal removal from synthetic effluents was assessed using neutron-activation analysis at the IBR-2 reactor (JINR, Dubna, Russia). To determine copper content, samples were irradiated for 1 min and measured immediately after irradiation for 15 min. To determine silver, nickel and zinc, content samples were irradiated for 3 days and measured for 1.5 h after 20 days of irradiation. The analysis of the spectra and calculation of metal concentrations was done using the Genie2000 software (2000, Canberra, Meriden, CT, USA) and “Concentration” (Version 9, JINR, Dubna, Russia) software.

Biofilm formation on the zeolite was proved using a laser confocal scanning microscope (Leica SP5, Berlin, Germany). Polysaccharide matrix was stained with lectin IV from wheat germ agglutinin (WGA, Sigma-Aldrich, Darmstadt, Germany) conjugated with fluorescent dye Alexa Fluor 488 (W11261 ThermoFisher, Waltham, MA, USA). For cell visualization, fluorescent dye SYTO[®] 11 (S7573 ThermoFisher, Waltham, MA, USA) diluted 1:1000 in

phosphate buffer (Sigma-Aldrich, Darmstadt, Germany) was applied. The Imaris software package (Version 7.0.0, Bitplane, Zurich, Switzerland) was applied to determine the area occupied by bacterial cells and polysaccharide matrix.

Infrared spectra of biosorbent before and after the adsorption process were obtained using the Nicolet 6700 spectrometer (Thermo Scientific, Waltham, MA, USA) with a zinc selenide ATR crystal. Samples were analysed without any preliminary pre-treatment.

3. Results

To prove formation of biofilm on the zeolite surface, the confocal laser scanning microscope was used. Images of raw zeolite and *S. xiamenensis* biofilm formed on zeolite (Figure 1) showed a small number of bacteria on the raw zeolite whereas the surface of modified zeolite was almost completely covered by biofilm (84%). Biofilm consisted mainly of polysaccharides (86.4%) and bacterial cells (13.6%).

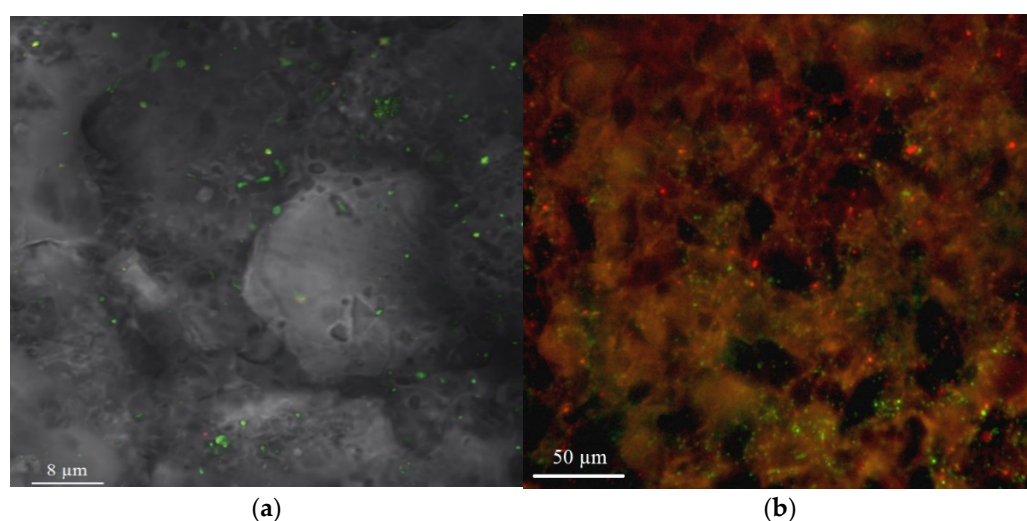


Figure 1. (a) Raw and (b) *S. xiamenensis* biofilm formed on zeolite.

3.1. Effect of pH on Metal Biosorption on Bio-Zeolite

As an important factor, pH exhibits a significant role in the metal ions removal using different type of sorbents [34]. In the analysed systems, metal removal by bio-zeolite increased with increasing pH (Figure 2). Thus, in the Ag-system, removal of silver ions increased from 15.5 % at pH 2.0 to 70 to 71% at pHs 5.0 to 6.0. At low pH values, the protonation of the functional groups of the bio-zeolite surface restrict binding of positively charged silver ions as a result of repulsive force. However, with the increase of pH, more functional groups on the biosorbent became negatively charged facilitating sorption of cations [35,36]. Silver ions at the studied pH range are present in solution Ag (I), while AgOH is generated at pH higher than 6.0 [2].

According to literature data, maximum removal of Ag(I) by activated carbon prepared from almond shell was achieved at pH 4.5 [37]. Silver sorption on *Myxococcus xanthus* biomass was studied at pH 5.5 [38]. The optimum pH for silver adsorption on the Japanese natural clinoptilolite was determined to be around 4.0 [39]. Silver removal by waste yeast and Spirulina biomass reached a maximum at pH 3.0 [2,40].

In the Ag-Cu system, an increase of the pH values also facilitated metal ions removal. For silver, the maximum removal of 55% was achieved at pH 5.0, and for copper, of 87% at pH 4.0 to 5.0. In comparison with the Ag-system, the removal of silver ions was reduced by 15%, indicating possible competition of silver and copper ions for binding sites.

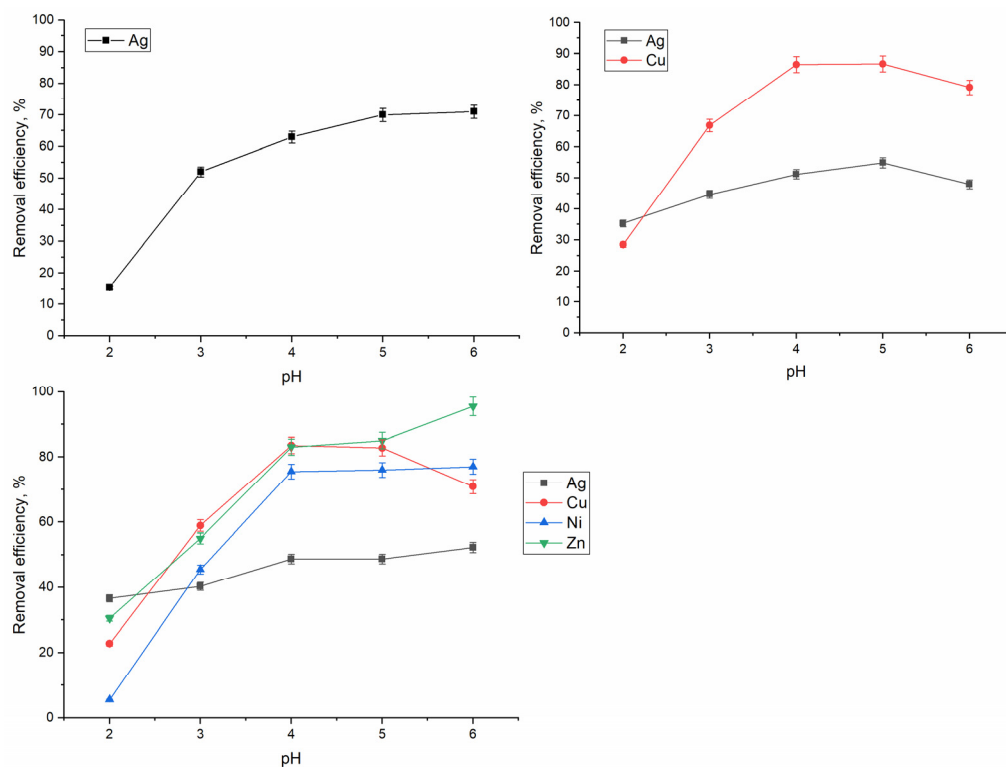


Figure 2. Influence of pH on silver, copper, nickel and zinc removal from studied synthetic solutions by bio-zeolite (time: 1 h, temperature: 20 °C, pH: 2.0–6.0, $C_{i,Ag}$: 10 mg/L, $C_{i,Cu}$: 5 mg/L, $C_{i,Ni}$, Zn : 2 mg/L).

In the Ag-Cu-Ni-Zn system, as in previously described systems, an increase of pH promoted metal ions removal. Maximum removal of silver, nickel and zinc was attained at pH 6.0: 52, 77 and 95%, respectively. It should be noted that nickel removal was almost on the same level at pH range 4.0–6.0 and constituted 75–77%. pH 4.0–5.0 was more favourable for copper ions removal, when 83% of ions were extracted from the solution.

3.2. Effect of Time on Metal Biosorption on Bio-Zeolite and Kinetic Studies

The kinetics of the metal ions biosorption on the bio-zeolite were investigated and the results are presented in Figures 3–5. The process of silver ions removal was relatively fast and equilibrium was attained within 90 min in the Ag-system, 30 min in the Ag-Cu system and 120 min in the Ag-Cu-Ni-Zn system. Maximum silver ions removal in the analysed systems constituted 72, 70 and 52%, respectively. Equilibrium for silver sorption on waste yeast was reached within 60 min [2].

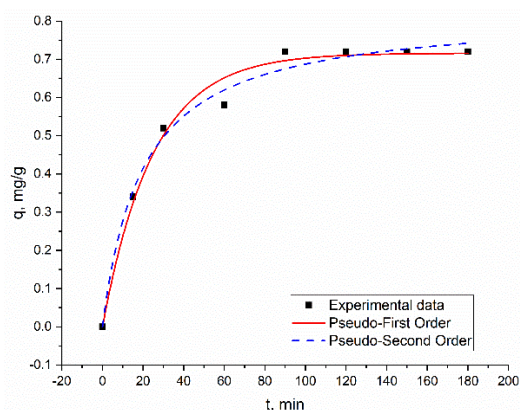


Figure 3. The kinetic curves for silver ions’ sorption on bio-zeolite in Ag-system.

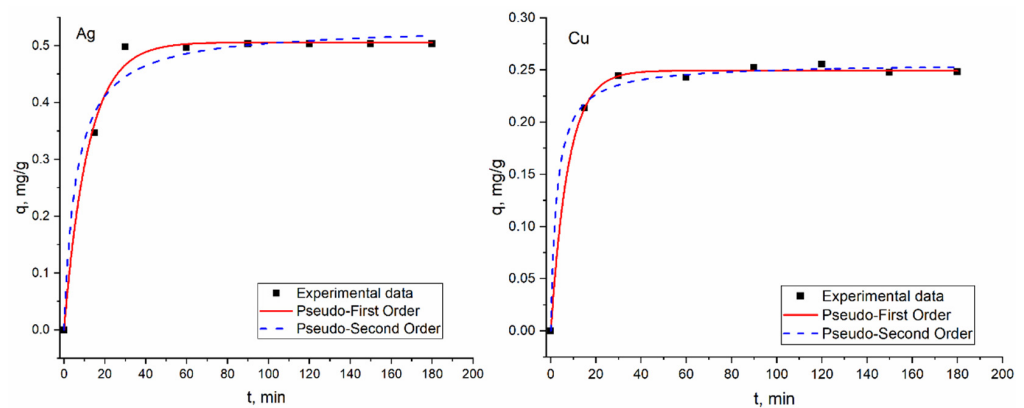


Figure 4. The kinetic curves for silver and copper ions' sorption on bio-zeolite in Ag-Cu system.

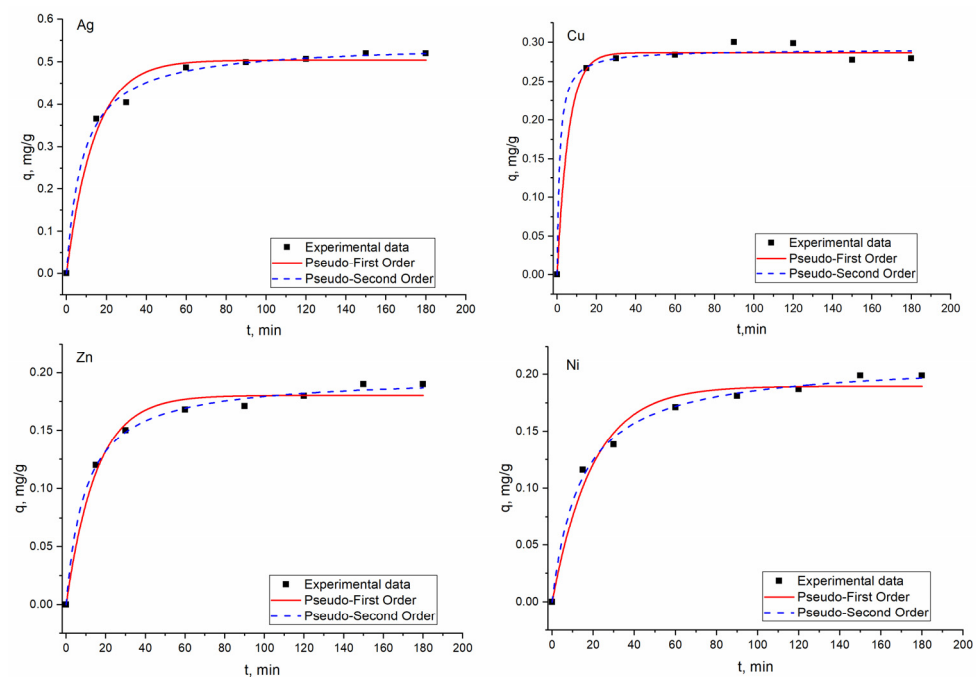


Figure 5. The kinetic curves for silver, copper, nickel and zinc ions' sorption on bio-zeolite in the Ag-Cu-Ni-Zn system.

In the binary (Ag-Cu) system, 77% of Cu were removed from the solution in 60 min of sorbent-sorbate interaction, while in the quaternary system, 83% of copper ions were removed in 150 min. The maximum removal of zinc and nickel ions was attained in 150 min, when 95% of zinc and 100% of nickel ions were removed from the solution. The process of metal sorption took place in two stages: fast sorption, followed by a slow stage with equilibrium achievement. A drastic increase of metal ions sorption at the first stage is explained by the large number of the vacant sites of the bio-zeolite surface. Lowering the sorption in the next stage is mainly due to saturation of the binding sites and attainment of equilibrium [36,41]. Fast adsorption at the first stage can be also explained by metal ions trapping to the exterior surface, while the metal ions' entrance into the pores (interior surface) is a relatively slow process [36].

Data obtained experimentally were fitted to pseudo-first-order (PFO) and pseudo-second-order models described by the following equations:

The pseudo-first-order model (PFO) considers that the rate of occupation of the adsorption sites is proportional to the number of unoccupied sites [42]:

$$q_t = q_e (1 - e^{-k_1 t}) \quad (3)$$

where q_e and q_t are the quantities of metal (mg/g) adsorbed from the solution at equilibrium and at any time t (min), respectively, and k_1 (1/min) is the rate constant of the pseudo-first-order model.

The pseudo-second-order model (PSO) shows that chemical absorption is one of the mechanisms of metal sorption onto sorbent:

$$q = \frac{q_e^2 k_2 t}{1 + q_e k_2 t} \quad (4)$$

where k_2 (g/mg·min) is the rate constant of the pseudo-second-order model.

The applicability of kinetic models was confirmed by SSE (sum of error squares), %:

$$SSE = \frac{\sqrt{\sum (q_{e, cal} - q_{e, exp})^2}}{N} \quad (5)$$

where N is the number of experimental points.

One more parameter calculated to prove the applicability of the models was adjusted R squared:

$$R_{adj}^2 = 1 - (1 - R^2) \left[\frac{n - 1}{n - (k + 1)} \right] \quad (6)$$

where R^2 was obtained from the applied models, K is the number of predictors and n is the number of experimental values.

The kinetic data of metal ions adsorption onto bio-zeolite calculated from the related non-linear fitting curves (Figures 3–5) are listed in Table 2.

Table 2. Parameters calculated from pseudo-first-order (PFO) and pseudo-second-order models.

	Metal	Ag	Ag-Cu		Ag-Cu-Ni-Zn			
		Ag	Ag	Cu	Ag	Cu	Ni	Zn
PFO	q_{exp} , mg/g	0.72 ± 0.02	0.50 ± 0.003	0.25 ± 0.03	0.52 ± 0.01	0.28 ± 0.003	0.20 ± 0.004	0.19 ± 0.003
	q_e , mg/g	0.71 ± 0.01	0.50 ± 0.006	0.25 ± 0.01	0.50 ± 0.01	0.28 ± 0.003	0.19 ± 0.005	0.18 ± 0.004
	k_1 , min ⁻¹	0.04 ± 0.004	0.08 ± 0.007	0.13 ± 0.07	0.07 ± 0.008	0.17 ± 0.03	0.05 ± 0.006	0.07 ± 0.007
	R^2	0.98	0.99	0.99	0.98	0.99	0.97	0.97
	R_{adj}^2	0.99	0.99	0.98	0.96	0.97	0.95	0.96
	SSE, %	0.09	0.08	0.39	0.08	0.02	0.90	0.2
PSO	q_e , mg/g	0.82 ± 0.02	0.53 ± 0.01	0.25 ± 0.01	0.54 ± 0.008	0.28 ± 0.005	0.21 ± 0.004	0.20 ± 0.003
	k_2 , g/mg·min	0.06 ± 0.001	0.03 ± 0.009	1.48 ± 0.009	0.3 ± 0.002	2.7 ± 0.01	0.3 ± 0.03	0.05 ± 0.05
	R^2	0.99	0.98	0.99	0.99	0.99	0.99	0.99
	R_{adj}^2	0.99	0.98	0.98	0.98	0.98	0.98	0.99
	SSE	0.16	0.18	0.51	0.10	0.01	1.0	0.2

The experimentally obtained (q_{exp}) and calculated ($q_{e, cal}$) values of sorption capacity for both models were very close, confirming their suitability for explanation of experimentally obtained data. Comparing the coefficient of determination values for silver, it was found that they were higher for the PSO model in Ag- and Ag-Cu-Ni-Zn systems, assuming that the adsorption was a chemisorption process [14]. The Akaike Information Criterion (AIC) test confirmed these results. In the case of the Ag-Cu system, silver absorption was better described by the PFO model. According to the AIC test, the PFO model also showed itself to be more applicable for describing copper ions sorption in both systems containing copper ions. The PSO model fitted well data for nickel and zinc ions in the Ag-Cu-Ni-Zn system. Zhao and co-authors [2] suggested that ion exchange, chelating sorption and redox by active protons on the sulfo, amino and hydroxyl groups played a major role in silver sorption on the microbial biomass.

3.3. Effect of Silver Concentration on Its Biosorption on Bio-Zeolite and Equilibrium Studies

Increase of the initial metal concentration in solution is usually associated with an increase in the sorbents adsorption capacity since it provides a driving force to overcome all mass transfer resistances of metal ions between aqueous and solid phase [36]. Studying the effect of silver concentration on bio-zeolite adsorption capacity, it was shown that it increased with increasing metal concentration, and the maximum adsorption was achieved at an initial concentration of 100 mg/L. Thus, the maximum silver sorption was 5.83 mg/g in the Ag-system, 7.79 mg/g in the Ag-Cu system and 7.22 mg/g in the Ag-Cu-Ni-Zn system (Figure 6). Higher silver sorption in complex systems can be explained by the synergetic effect of the biofilm that, after ion enrichment, allows entrance of the metal ions to deeper sites of the support, thereby liberating external surface sites [43].

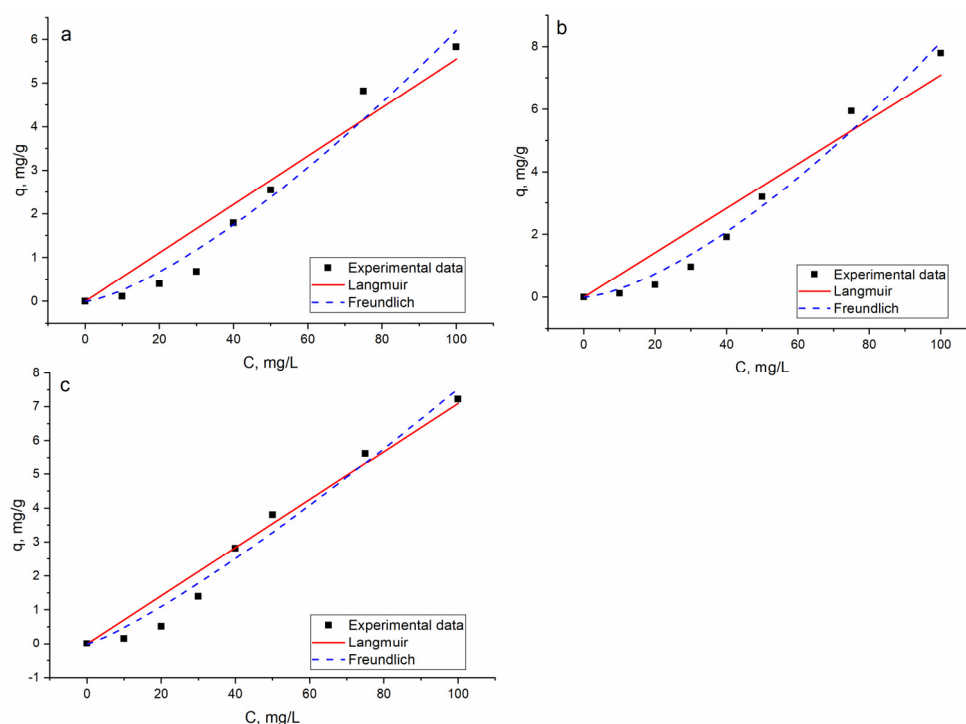


Figure 6. The sorption isotherms for silver adsorption on the bio-zeolite: (a) Ag (b) Ag-Cu and (c) Ag-Cu-Ni-Zn systems.

As was mentioned previously, the concentration of other metal ions in the solution was maintained as a constant. Increase of silver concentration in solution did not influence removal of copper ions in the Ag-Cu system; it was almost at the same level at all applied silver concentrations. Thus, it can be concluded that silver and copper ions are fixed by different functional groups. It is interesting to note that in the presence of copper ions in the solution, adsorption of silver ions increased compared to the Ag-system. In the Ag-Cu-Ni-Zn system, the efficiency of copper removal was not affected by an increase of silver concentration, while removal of nickel and zinc was reduced by 24 and 30%, respectively. This may indicate competition of silver, zinc and nickel for binding sites.

Langmuir and Freundlich isotherms generally used to fit equilibrium adsorption data are expressed by Equations (6) and (7). The Langmuir model assumes a monolayer coverage of adsorbate on the homogeneous surface, while applicable to adsorption processes that occur on heterogeneous surfaces [44].

$$q_e = \frac{q_m b C_e}{1 + b C_e} \quad (7)$$

where q_m (mg/g) is the maximum adsorption capacity of the bio-zeolite, C_e (mg/L) is the metal concentration at the equilibrium on the aqueous media and b is the adsorption equilibrium constant (L/mg).

$$q_e = K_F C_e^{\frac{1}{n}} \quad (8)$$

where K_F (L/mg) and n are the constants of adsorption affinity.

The plots of the non-linear fitting curves of the Langmuir and Freundlich models are presented in Figure 6 and the corresponding parameters are given in Table 3.

Table 3. The parameters of the Langmuir and Freundlich models.

		Ag	Ag-Cu	Ag-Cu-Ni-Zn
Langmuir	q_m , mg/g	14.8 ± 0.08	32.5 ± 0.5	12.8 ± 0.05
	b , L/mg	0.38 ± 0.003	0.22 ± 0.003	0.50 ± 0.002
	R_L	0.02	0.04	0.02
	R^2	0.92	0.91	0.96
	R_{adj}^2	0.90	0.90	0.95
Freundlich	K_F , mg/g	0.01 ± 0.007	0.008 ± 0.0006	0.03 ± 0.001
	$1/n$	1.39 ± 0.08	1.49 ± 0.06	1.2 ± 0.01
	R^2	0.97	0.98	0.97
	R_{adj}^2	0.96	0.97	0.96

According to the R^2 and AIC test, the Freundlich model was more suitable for the description of experimentally obtained values in all analysed systems, indicating that adsorption processes occurs on heterogeneous surfaces. The values of R_L from the Langmuir model in the range between 0 and 1 and $1/n$ from the Freundlich in the range of 1–10 confirm the favourable conditions for sorption. In addition, since n values in the present study were higher than 1.0, chemical absorption can be considered dominant for silver ions' sorption [45]. The theoretical maximum adsorption capacity calculated from Langmuir model ranged from 12.8 in the Ag-Cu-Ni-Zn system to 32.5 mg/g in the Ag-Cu system.

The biosorption of silver by a waste product from the alginate production industry was also better described by the Freundlich model [1]. The Langmuir model fitted the experimental data better than that of the Freundlich model in the case of silver biosorption by waste yeast [2].

The comparison of the sorption capacity of the bio-zeolite with data reported for other type of sorbents is presented in Table 4. The bio-zeolite sorption capacity was comparable with sorption capacity of biological origin and lower than those of synthetic sorbents.

Table 4. Adsorptive capacity of different types of sorbents in silver ions' removal.

Sorbent	q_{max} , mg/g	Concentrations Range, mg/L	pH	Reference
Bio-zeolite	12.8–32.5	10–100	6.0	Present study
Fe ₃ O ₄ @SiO ₂ @TiO ₂ -IIP	30.55	10–300	6.0	[11]
Fe ₃ O ₄ @SiO ₂ @TiO ₂ -NIP	17.21	10–300	6.0	[11]
Acidified biosorbent	2.92 mmol/g	10–200	5.0	[1]
Waste yeast	18.9–41.8	0–750	3.0	[2]
<i>Arthrospira platensis</i>	31.6	5–30	3.0	[40]
Poly(o-phenylenediamine) Microparticles	533	1–10 mM	5.0	[46]
Japanese Natural Clinoptilolite	0.64 mmol/g	50	4.0	[39]

3.4. Effect of Temperature on Silver Biosorption on Bio-Zeolite and Thermodynamic Studies

The temperature of the solution influenced the process of metal ions removal from analysed systems (Figure 7). Thus, in the Ag-system, a rise of temperature from 20 to 30 °C led to the decrease of bio-zeolite sorption capacity from 71 to 24%, then silver

removal increased up to 61% with a temperature increase up to 50 °C (Figure 7). The same pattern was observed in the Ag-Cu system: silver removal firstly decreased with a temperature increase to 30 °C, then it rose with the temperature growing and reached the value of 52% at 50 °C (it was very close to the removal capacity of 54% at 20 °C). Copper removal continuously decreased with the increase of temperature. In the Ag-Cu-Ni-Zn system, the behaviour of silver removal was similar to previously described systems, while removal of copper, nickel and zinc firstly increased up to a temperature of 40 °C and then was slightly reduced.

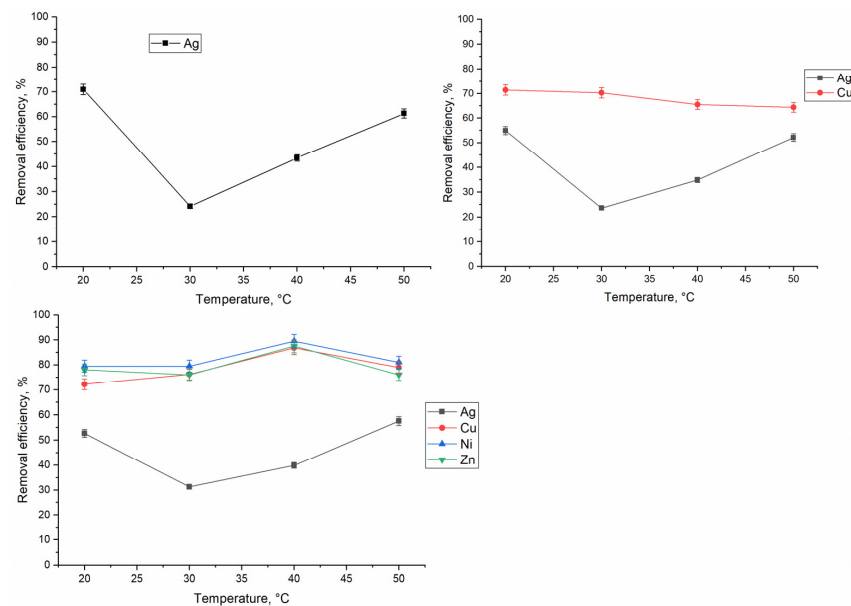


Figure 7. Effect of temperature on metal ions removal by bio-zeolite (time 1 h, temperature 20–50 °C, pH 5.0, $C_{i,Ag}$ 10 mg/L, $C_{i,Cu}$ 5 mg/L, $C_{i,Ni}$, Zn 2 mg/L).

The decrease of silver removal with temperature grown up to 30 °C can be associated with weakening of the structure of the biomass cell and even decomposition of the biomolecules that may lead to the reduction of the number of active binding sites [47]. It can be suggested that at higher temperatures, silver ions are mainly adsorbed on the zeolite surface. As the temperature increased, molecular vibrations begin to terminate intrinsic bonds of water molecules on the surface of zeolite due to the heat energy, and more binding sites are available for metal removal [48].

The thermodynamic parameters ΔG° , ΔH° , and ΔS° were calculated from the following Equations (9)–(11):

$$\ln K_d = \frac{\Delta S^\circ}{R} - \frac{\Delta H^\circ}{RT} \quad (9)$$

$$\Delta G^\circ = \Delta H^\circ - T\Delta S^\circ \quad (10)$$

where K_d is the distribution coefficient and it is calculated according to Equation (10):

$$K_d = \frac{(C_0 - C_e)V}{mC_e} \quad (11)$$

where ΔH° (J/mol) and ΔS° , J/mol K are enthalpy and entropy changes, respectively, R is the universal gas constant, 8.314 J/mol K, and T is the absolute temperature, K .

The enthalpy and entropy values were calculated by a plot of $\ln K_d$ versus $1/T$ (Supplementary Figure S1), and the corresponding thermodynamic parameters are given in Table 5. The values of ΔG° for all elements in analysed systems were negative, exhibiting that the adsorption was a spontaneous process. The positive value of ΔS° for all elements suggests the increased randomness at the liquid–solid interface during metal ions adsorption likely

indicates the process is an entropy-driven process rather than enthalpy [14]. The low value of ΔS° indicated that no remarkable change in entropy occurred during the adsorption process [36].

Table 5. Thermodynamic parameters for metal ions sorption on bio-zeolite.

System	Metal	ΔG° , kJ/mol				ΔH° , kJ/mol	ΔS° , J/mol·K	R^2
		293 K	303 K	313 K	323 K			
Ag	Ag	−9.3	−9.6	−10.0	−10.3	0.4	33	0.79
Ag-Cu	Ag	−8.8	−9.1	−9.5	−9.8	1.2	34	0.88
	Cu	−10.5	−10.7	−11.0	−11.3	−2.4	27.4	
Ag-Cu-Ni-Zn	Ag	−9.3	−9.6	−9.8	−10.1	−1.8	24.4	0.98
	Cu	−10.6	−11.0	−11.5	−11.9	2.3	44.0	0.99
	Ni	−9.2	−9.6	−10.0	−10.4	2.2	30.0	0.99
	Zn	−11.8	−12.1	−12.5	−12.9	−0.5	38.2	0.98

The positive values of ΔH° revealed the endothermic nature of the adsorption process for silver in Ag- and Ag-Cu systems as well as for copper and nickel in the Ag-Cu-Ni-Zn system. For other elements, negative values of ΔH° revealed the exothermic nature of the adsorption process. Since ΔH values were lower than 20.9 kJ/mol, it can be suggested that adsorption of elements in analysed systems belongs to physical adsorption [12].

3.5. FTIR Spectra

FTIR spectra were recorded in order to reveal involvement of functional groups of bio-zeolite in metals ions binding. According to Figure 8, in the control bio-zeolite, the bands at 760 and 1030 cm^{-1} attributed to O-Si-O and Si-O-Al groups were present [49]. Bands at 3610 cm^{-1} and deformation at area 1600 cm^{-1} are characteristic of -OH groups. In Ag-loaded biosorbent, the shift of identified groups by 10/15 cm^{-1} points at their involvement in silver ions removal. In the case of the Ag-Cu system, shifting of the band positions of Si-O- and -Si-O-Si- groups by 5/20 cm^{-1} and of -OH group by 5/7 cm^{-1} showed their involvement in silver and copper ions removal. In the multi-metal system, the shift of the bands of -Si-O- and -OH groups was observed. As possible mechanisms of metal ions sorption, one can regard the formation of bi- and mono-dentate ligands of metal ions with -OH groups and subsequent strong electrostatic interaction with a charged bio-zeolite surface [50].

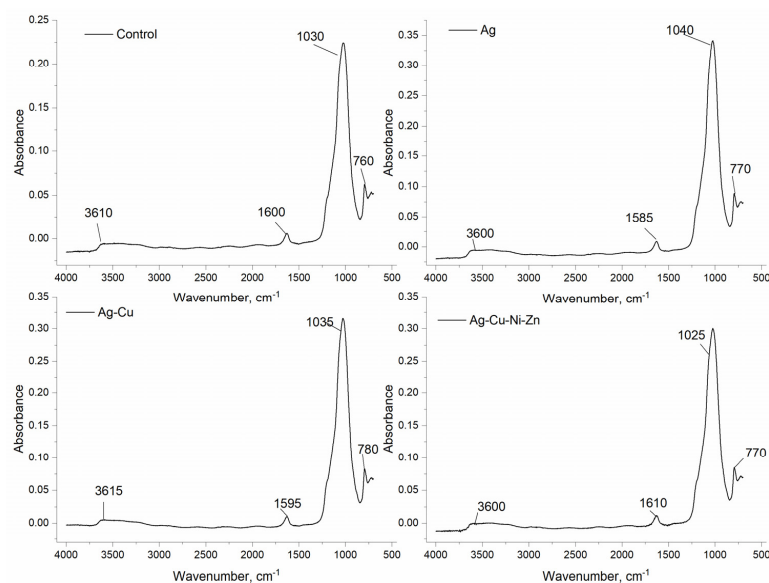


Figure 8. FTIR spectra of bio-zeolite before and after metal ions biosorption.

4. Conclusions

The zeolite with *Shewanella xiamenensis* biofilm was shown to be an effective adsorbent for the treatment of silver-containing effluents with different chemical composition. The adsorption of metal ions on bio-zeolite was pH dependent; the optimal pH for the highest metal removal was in the range of 4.0–6.0. The adsorption equilibrium experimental data fitted better with the pseudo-second-order model, except silver in the Ag-Cu system and copper in both systems. The adsorption isotherm fitted well with the Freundlich model, pointing out the predominant role of chemisorption in metal removal. The maximum adsorption capacity of bio-zeolite calculated from the Langmuir model reached 32.5 mg/g in the Ag-Cu system. The adsorption was shown to be as a spontaneous process endothermic or exothermic in nature depending on the metal ion, which is driven by entropy. Based on the data obtained in the present study, it can be concluded that metal ions' removal from silver-containing effluents by bio-zeolite is a physico-chemical adsorption process rather than a pure physical or chemical adsorption process.

Supplementary Materials: The following supporting information can be downloaded at: <https://www.mdpi.com/article/10.3390/min13020179/s1>, Figure S1: Plot of $\ln K_d$ versus $1/T$.

Author Contributions: Experimental design, I.Z. and N.Y.; sorbent preparation, A.S.; sorption experiment performance, I.Z. and N.Y.; sample irradiation and data processing, D.G. and I.Z.; sorbent analysis, A.S.; writing—original draft preparation, I.Z.; writing—review and editing, all authors. All authors have read and agreed to the published version of the manuscript.

Funding: This research received no external funding.

Data Availability Statement: Data are contained within the article or Supplementary Material.

Conflicts of Interest: The authors declare no conflict of interest.

References

1. de Freitas, G.R.; Vieira, M.G.A.; da Silva, M.G.C. Characterization and biosorption of silver by biomass waste from the alginate industry. *J. Clean. Prod.* **2020**, *271*, 122588. [[CrossRef](#)]
2. Zhao, Y.; Wang, D.; Xie, H.; Won, S.W.; Cui, L.; Wu, G. Adsorption of Ag (I) from aqueous solution by waste yeast: Kinetic, equilibrium and mechanism studies. *Bioprocess Biosyst. Eng.* **2014**, *38*, 69–77. [[CrossRef](#)] [[PubMed](#)]
3. Ratte, H.T. Bioaccumulation and toxicity of silver compounds: A review. *Environ. Toxicol. Chem.* **1999**, *18*, 89–108. [[CrossRef](#)]
4. Ferdous, Z.; Nemmar, A. Health Impact of Silver Nanoparticles: A Review of the Biodistribution and Toxicity Following Various Routes of Exposure. *Int. J. Mol. Sci.* **2020**, *21*, 2375. [[CrossRef](#)]
5. Drake, P.L.; Hazelwood, K.J. Exposure-Related Health Effects of Silver and Silver Compounds: A Review. *Ann. Occup. Hyg.* **2005**, *49*, 575–585. [[CrossRef](#)]
6. Zhang, J.; Wang, F.; Yalamarty, S.S.K.; Filipczak, N.; Jin, Y.; Li, X. Nano Silver-Induced Toxicity and Associated Mechanisms. *Int. J. Nanomed.* **2022**, *17*, 1851–1864. [[CrossRef](#)]
7. De Matteis, V. Exposure to Inorganic Nanoparticles: Routes of Entry, Immune Response, Biodistribution and In Vitro/In Vivo Toxicity Evaluation. *Toxics* **2017**, *5*, 29. [[CrossRef](#)]
8. Bakand, S.; Hayes, A. Toxicological Considerations, Toxicity Assessment, and Risk Management of Inhaled Nanoparticles. *Int. J. Mol. Sci.* **2016**, *17*, 929. [[CrossRef](#)]
9. Gao, Y.; Zhou, Y.; Wang, H.; Lin, W.; Wang, Y.; Sun, D.; Hong, J.; Li, Q. Simultaneous Silver Recovery and Cyanide Removal from Electroplating Wastewater by Pulse Current Electrolysis Using Static Cylinder Electrodes. *Ind. Eng. Chem. Res.* **2013**, *52*, 5871–5879. [[CrossRef](#)]
10. Elwakeel, K.Z.; Al-Bogami, A.S.; Guibal, E. 2-Mercaptobenzimidazole derivative of chitosan for silver sorption—Contribution of magnetite incorporation and sonication effects on enhanced metal recovery. *Chem. Eng. J.* **2020**, *403*, 126265. [[CrossRef](#)]
11. Yin, X.; Long, J.; Xi, Y.; Luo, X. Recovery of Silver from Wastewater Using a New Magnetic Photocatalytic Ion-Imprinted Polymer. *ACS Sustain. Chem. Eng.* **2017**, *5*, 2090–2097. [[CrossRef](#)]
12. Liu, H.; Zhang, F.; Peng, Z. Adsorption mechanism of Cr(VI) onto GO/PAMAMs composites. *Sci. Rep.* **2019**, *9*, 3663. [[CrossRef](#)] [[PubMed](#)]
13. Demey, H.; Vincent, T.; Guibal, E. A novel algal-based sorbent for heavy metal removal. *Chem. Eng. J.* **2018**, *332*, 582–595. [[CrossRef](#)]
14. Tighadouini, S.; Radi, S.; Roby, O.; Hammoudan, I.; Saddik, R.; Garcia, Y.; Almarhoon, Z.M.; Mabkhot, Y.N. Kinetics, thermodynamics, equilibrium, surface modelling, and atomic absorption analysis of selective Cu(II) removal from aqueous solutions and rivers water using silica-2-(pyridin-2-ylmethoxy)ethan-1-ol hybrid material. *RSC Adv.* **2021**, *12*, 611–625. [[CrossRef](#)]

15. Zinicovscaia, I.; Yushin, N.; Grozdov, D.; Vergel, K.; Nekhoroshkov, P.; Rodlovskaya, E. Treatment of Rhenium-Containing Effluents Using Environmentally Friendly Sorbent, *Saccharomyces cerevisiae* Biomass. *Materials* **2021**, *14*, 4763. [[CrossRef](#)] [[PubMed](#)]
16. Zinicovscaia, I.; Yushin, N.; Abdusamadzoda, D.; Grozdov, D.; Shvetsova, M. Efficient Removal of Metals from Synthetic and Real Galvanic Zinc-Containing Effluents by Brewer's Yeast *Saccharomyces cerevisiae*. *Materials* **2020**, *13*, 3624. [[CrossRef](#)]
17. Fathollahi, A.; Khasteganan, N.; Coupe, S.J.; Newman, A.P. A meta-analysis of metal biosorption by suspended bacteria from three phyla. *Chemosphere* **2021**, *268*, 129290. [[CrossRef](#)]
18. Pham, V.H.T.; Kim, J.; Chang, S.; Chung, W. Bacterial Biosorbents, an Efficient Heavy Metals Green Clean-Up Strategy: Prospects, Challenges, and Opportunities. *Microorganisms* **2022**, *10*, 610. [[CrossRef](#)]
19. Wang, J.; Chen, C. Biosorbents for heavy metals removal and their future. *Biotechnol. Adv.* **2009**, *27*, 195–226. [[CrossRef](#)]
20. Moghaddam, S.A.E.; Harun, R.; Mokhtar, M.N.; Zakaria, R. Potential of Zeolite and Algae in Biomass Immobilization. *BioMed Res. Int.* **2018**, *2018*, 6563196. [[CrossRef](#)]
21. Vijayaraghavan, K.; Yun, Y.-S. Bacterial biosorbents and biosorption. *Biotechnol. Adv.* **2008**, *26*, 266–291. [[CrossRef](#)]
22. Yuna, Z. Review of the Natural, Modified, and Synthetic Zeolites for Heavy Metals Removal from Wastewater. *Environ. Eng. Sci.* **2016**, *33*, 443–454. [[CrossRef](#)]
23. Elboughdiri, N. The use of natural zeolite to remove heavy metals Cu (II), Pb (II) and Cd (II), from industrial wastewater. *Cogent Eng.* **2020**, *7*, 1782623. [[CrossRef](#)]
24. Erdem, E.; Karapinar, N.; Donat, R. The removal of heavy metal cations by natural zeolites. *J. Colloid Interface Sci.* **2004**, *280*, 309–314. [[CrossRef](#)]
25. Senila, L.; Hoaghia, A.; Moldovan, A.; Török, I.A.; Kovacs, D.; Simedru, D.; Tomoiag, C.H.; Senila, M. The Potential Application of Natural Clinoptilolite-Rich Zeolite as Support for Bacterial Community Formation for Wastewater Treatment. *Materials* **2022**, *15*, 3685. [[CrossRef](#)] [[PubMed](#)]
26. Popova, N.; Artemiev, G.; Zinicovscaia, I.; Yushin, N.; Demina, L.; Boldyrev, K.; Sobolev, D.; Safonov, A. Biogeochemical Permeable Barrier Based on Zeolite and Expanded Clay for Immobilization of Metals in Groundwater. *Hydrology* **2022**, *10*, 4. [[CrossRef](#)]
27. Zinicovscaia, I.; Yushin, N.; Grozdov, D.; Abdusamadzoda, D.; Safonov, A.; Rodlovskaya, E. Zinc-Containing Effluent Treatment Using *Shewanella xiamenensis* Biofilm Formed on Zeolite. *Materials* **2021**, *14*, 1760. [[CrossRef](#)]
28. Khosravi, A.; Javdan, M.; Yazdanpanah, G.; Malakootian, M. Removal of heavy metals by *Escherichia coli* (*E. coli*) biofilm placed on zeolite from aqueous solutions (case study: The wastewater of Kerman Bahonar Copper Complex). *Appl. Water Sci.* **2020**, *10*, 167. [[CrossRef](#)]
29. Silva, B.; Pimentel, C.Z.; Machado, B.; Costa, F.; Tavares, T. Performance of a Combined Bacteria/Zeolite Permeable Barrier on the Rehabilitation of Wastewater Containing Atrazine and Heavy Metals. *Processes* **2023**, *11*, 246. [[CrossRef](#)]
30. Monge-Amaya, O.; Valenzuela-García, J.L.; Félix, E.A.; Certucha-Barragan, M.T.; Leal-Cruz, A.L.; Almendariz-Tapia, F.J. Biosorptive Behavior of Aerobic Biomass Biofilm Supported on Clinoptilolite Zeolite for the Removal of Copper. *Miner. Process. Extr. Met. Rev.* **2013**, *34*, 422–428. [[CrossRef](#)]
31. Quintelas, C.; Rocha, Z.; Silva, B.; Fonseca, B.; Figueiredo, H.; Tavares, T. Biosorptive performance of an *Escherichia coli* biofilm supported on zeolite NaY for the removal of Cr(VI), Cd(II), Fe(III) and Ni(II). *Chem. Eng. J.* **2009**, *152*, 110–115. [[CrossRef](#)]
32. Gu, J.-N.; Liang, J.; Chen, C.; Li, K.; Zhou, W.; Jia, J.; Sun, T. Treatment of real deplating wastewater through an environmental friendly precipitation-electrodeposition-oxidation process: Recovery of silver and copper and reuse of wastewater. *Sep. Purif. Technol.* **2020**, *248*, 117082. [[CrossRef](#)]
33. Grouzdev, D.S.; Safonov, A.V.; Babich, T.L.; Tourova, T.P.; Krutkina, M.S.; Nazina, T.N. Draft Genome Sequence of a Dissimilatory U(VI)-Reducing Bacterium, *Shewanella xiamenensis* Strain DCB2-1, Isolated from Nitrate- and Radionuclide-Contaminated Groundwater in Russia. *Genome Announc.* **2018**, *6*, e00555-18. [[CrossRef](#)] [[PubMed](#)]
34. Huang, J.; Yuan, F.; Zeng, G.; Li, X.; Gu, Y.; Shi, L.; Liu, W.; Shi, Y. Influence of pH on heavy metal speciation and removal from wastewater using micellar-enhanced ultrafiltration. *Chemosphere* **2017**, *173*, 199–206. [[CrossRef](#)]
35. Wei, W.; Wang, Q.; Li, A.; Yang, J.; Ma, F.; Pi, S.; Wu, D. Biosorption of Pb (II) from aqueous solution by extracellular polymeric substances extracted from *Klebsiella* sp. J1: Adsorption behavior and mechanism assessment. *Sci. Rep.* **2016**, *6*, 31575. [[CrossRef](#)] [[PubMed](#)]
36. Chowdhury, S.; Mishra, R.; Kushwaha, P.; Saha, P. Removal of safranin from aqueous solutions by NaOH-treated rice husk: Thermodynamics, kinetics and isosteric heat of adsorption. *Asia-Pac. J. Chem. Eng.* **2010**, *7*, 236–249. [[CrossRef](#)]
37. Omri, A.; Benzina, M. Adsorption characteristics of silver ions onto activated carbon prepared from almond shell. *Desalination Water Treat.* **2013**, *51*, 2317–2326. [[CrossRef](#)]
38. Merroun, M.L.; Ben Omar, N.; Alonso, E.; Arias, J.M.; González-Muñoz, M.T. Silver sorption to *Myxococcus xanthus* biomass. *Geomicrobiol. J.* **2001**, *18*, 183–192. [[CrossRef](#)]
39. Wajima, T. Removal of Ag(I) from Aqueous Solution by Japanese Natural Clinoptilolite. *Adv. Chem. Eng. Sci.* **2016**, *6*, 470–487. [[CrossRef](#)]
40. Zinicovscaia, I.; Cepoi, L.; Chiriac, T.; Mitina, T.; Grozdov, D.; Yushin, N.; Culicov, O. Application of *Arthrospira* (*Spirulina*) *platensis* biomass for silver removal from aqueous solutions. *Int. J. Phytoremediat.* **2017**, *19*, 1053–1058. [[CrossRef](#)]
41. Patel, H. Batch and continuous fixed bed adsorption of heavy metals removal using activated charcoal from neem (*Azadirachta indica*) leaf powder. *Sci. Rep.* **2020**, *10*, 16895. [[CrossRef](#)] [[PubMed](#)]

42. Cruz, C.C.; da Costa, A.C.A.; Henriques, C.A.; Luna, A.S. Kinetic modeling and equilibrium studies during cadmium biosorption by dead *Sargassum* sp. biomass. *Bioresour. Technol.* **2003**, *91*, 249–257. [[CrossRef](#)] [[PubMed](#)]
43. Lameiras, S.; Quintelas, C.; Tavares, T. Biosorption of Cr (VI) using a bacterial biofilm supported on granular activated carbon and on zeolite. *Bioresour. Technol.* **2008**, *99*, 801–806. [[CrossRef](#)] [[PubMed](#)]
44. Ayawei, N.; Ebelegi, A.N.; Wankasi, D. Modelling and Interpretation of Adsorption Isotherms. *J. Chem.* **2017**, *2017*, 3039817. [[CrossRef](#)]
45. Chou, W.-L.; Wang, C.-T.; Chang, W.-C.; Chang, S.-Y. Adsorption treatment of oxide chemical mechanical polishing wastewater from a semiconductor manufacturing plant by electrocoagulation. *J. Hazard. Mater.* **2010**, *180*, 217–224. [[CrossRef](#)] [[PubMed](#)]
46. Li, X.-G.; Ma, X.-L.; Sun, J.; Huang, M.-R. Powerful Reactive Sorption of Silver(I) and Mercury(II) onto Poly(*o*-phenylenediamine) Microparticles. *Langmuir* **2009**, *25*, 1675–1684. [[CrossRef](#)]
47. Gupta, H.; Gogate, P.R. Intensified removal of copper from waste water using activated watermelon based biosorbent in the presence of ultrasound. *Ultrason. Sonochem.* **2016**, *30*, 113–122. [[CrossRef](#)]
48. Kaur, M.; Sharma, P.; Kumari, S. Equilibrium studies for copper removal from aqueous solution using nanoadsorbent synthesized from rice husk. *SN Appl. Sci.* **2019**, *1*, 988. [[CrossRef](#)]
49. Treto-Suárez, M.A.; Prieto-García, J.O.; Mollineda-Trujillo, Á.; Lamazares, E.; Hidalgo-Rosa, Y.; Mena-Ulecia, K. Kinetic study of removal heavy metal from aqueous solution using the synthetic aluminum silicate. *Sci. Rep.* **2020**, *10*, 10836. [[CrossRef](#)]
50. Baldermann, A.; Griebbacher, A.C.; Baldermann, C.; Purgstaller, B.; Letofsky-Papst, I.; Kaufhold, S.; Dietzel, M. Removal of Barium, Cobalt, Strontium, and Zinc from Solution by Natural and Synthetic Allophane Adsorbents. *Geosciences* **2018**, *8*, 309. [[CrossRef](#)]

Disclaimer/Publisher’s Note: The statements, opinions and data contained in all publications are solely those of the individual author(s) and contributor(s) and not of MDPI and/or the editor(s). MDPI and/or the editor(s) disclaim responsibility for any injury to people or property resulting from any ideas, methods, instructions or products referred to in the content.